Inorganic Chemistry

Article

pubs.acs.org/IC

Cr−Cr Quintuple Bonds: Ligand Topology and Interplay Between Metal−Metal and Metal−Ligand Bonding

Andrés Falceto,[†] Klaus H. Theopold,*[,‡] and Santiago Alvarez*[,†]

[†]Departament de Química Inorgànica and Institut de Química Teòrica i Computacional, Universitat de Barcelona, Martí i Franquès 1, 08028 Barcelona, Spain

[‡]Department of Chemistry and Biochemistry, Center for Catalytic Science and Technology, University of Delaware, Newark, Delaware 19716, United States

Supporting Information

ABSTRACT: Chromium−chromium quintuple bonds seem to be approaching the lower limit for their bond distances, and this computational density functional theory study tries to explore the geometrical and electronic factors that determine that distance and to find ways to fine-tune it via the ligand choice. While for monodentate ligands the Cr−Cr distance is predicted to shorten as the Cr−Cr−L bond angle increases, with bridging bidentate ligands the trend is the opposite, since those ligands with a larger number of spacers between the donor atoms favor larger bond angles and longer bond distances. Compared to Cr−Cr quadruple bonds, the quintuple bonding in Cr_2L_2 compounds (with L a bridging bidentate N-donor ligand) involves a sophisticated mechanism that comprises a positive pyramidality effect for the σ and one π bond, but a negative effect for one of the δ bonds. Moreover, the shorter Cr−Cr distances produce a mismatch of the bridging ligand lone pairs and the metal acceptor orbitals, which results in a negative correlation of the Cr−Cr and Cr−N bond distances in both experimental and calculated structures.

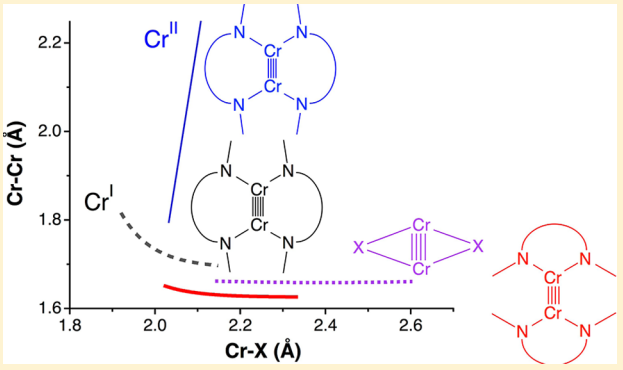

INTRODUCTION

The first coordination compounds featuring metal−metal quintuple bonds were introduced by Power and co-workers in 2005.[1] In those complexes each of the two chromium(I) centers is coordinated by the central phenyl ring of a terphenyl ligand and via a secondary coordinative π interaction by a flanking arene of the ligand σ-bonded to the other chromium atom (Scheme 1a). Other families of Cr_2L_2 complexes with shorter Cr−Cr bonds followed, starting with the diazadiene complex (Scheme 1b) made in the laboratory of Theopold,[2] even if the noninnocent nature of the ligands introduces some ambiguity as far as the formal Cr−Cr bond order is concerned. More recently, families that incorporate ligands with NCN backbones have been introduced: amidinates (Scheme 1c), pyridylamides (Scheme 1d), and guanidinates (Scheme 1e), synthesized by the groups of Tsai[3] and Kempe.[4] An amidinato complex with the Cr_2L_3 stoichiometry has been shown to present a similarly short Cr−Cr bond as well.[5] Related molybdenum complexes have also been prepared and characterized.[6] Finally, Lu et al. have recently published the first heterobinuclear complex featuring a Cr−Mn quintuple bond.[7] Progress in this field has been reviewed with some regularity.[3,4,8]

Not surprisingly, the characterization of Cr−Cr bonds with shorter distances and higher bond orders has boosted experimental and theoretical research.[9] However, so far the quintuple bonds seem to present a narrower range of distances (1.71[10]−1.84 Å, see Scheme 1) than the related Cr−Cr quadruple bonds, which span a range from 1.77[11] to 2.53 Å.[12] Therefore, there is ongoing interest in the search for the lower limit of a metal−metal bond distance. For systems with lower metal−metal bond orders, we have shown that short bond distances are associated with large M−M−L bond angles, what we called a pyramidality effect.[13] It affects metal−metal bonds of all bond orders,[14] and even noncovalent d^8−d^8 interactions.[15] This effect arises because bending the ligands away from the metal−metal bond favors hybridization of the σ- and π-bonding d orbitals by mixing in the p orbitals, thus strengthening the metal−metal bonds.[13a,b] In the lantern-type carboxylato-bridged Cr(II) complexes, the orbital pyramidality effect is less obvious because the bond angle and bond distance are not geometrically independent given the nearly rigid nature of the carboxylato bridges, but there is no doubt about the purely electronic pyramidality effect for quadruply bonded systems with nonbridging ligands as well as for the intermolecular contacts between d^8 square planar centers. In the present work we explore via density functional theory

Received: September 7, 2015
Published: October 26, 2015

DOI: 10.1021/acs.inorgchem.5b02059
Inorg. Chem. 2015, 54, 10966−10977

Scheme 1. Types of Ligands Supporting Cr−Cr Quintuple Bonds: (a) Terphenyl, (b) Diazadiene, (c) Amidinate, (d) Pyridylamides, and (e) Guanidinates

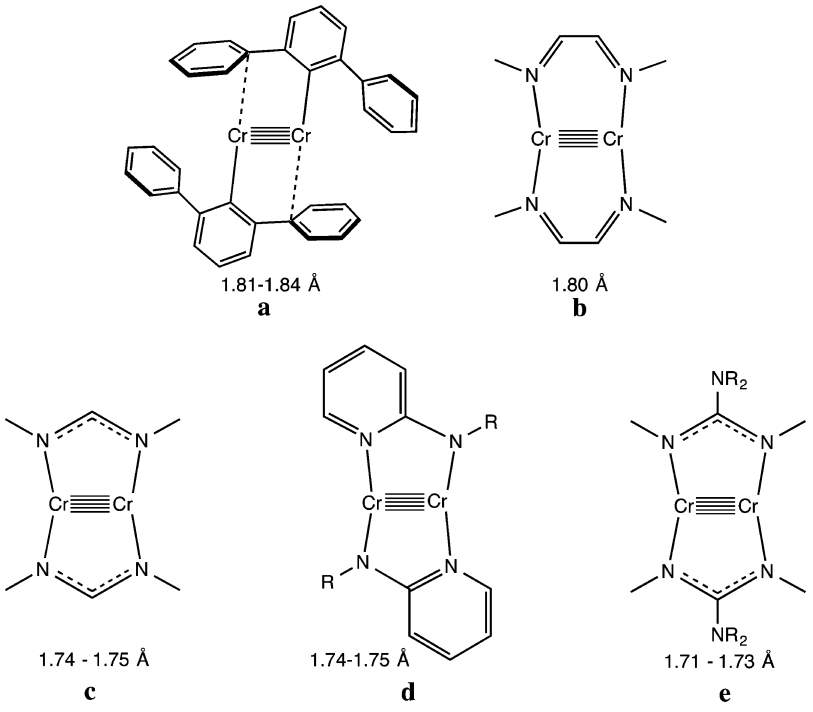

(DFT) calculations the possible existence of a pyramidality effect for Cr−Cr quintuple bonds, and we analyze how the ligand topology and chemical composition may affect the bond distances.

RESULTS AND DISCUSSION

Bond Angle-Bond Distance Correlation. Since bending the ligands away from the metal−metal bond favors rehybridization of the σ and π type d orbitals and strengthens metal−metal quadruple bonds,[13a,b] we have analyzed the effect of the Cr−Cr−L bond angle (α) on the Cr−Cr bond distance in Cr(I) model compounds with monodentate ligands, free of any constraints imposed by bridging ligands. The models used are planar $[Cr_2Me_4]^{2-}$, $[Cr_2(CN)_4]^{2-}$, and $[Cr_2(NH_3)_4]^{2+}$, and staggered $[Cr_2(NH_3)_6]^{2+}$, all in the singlet state. In all cases the Cr−Cr distance is shortened as the bond angle increases (Figure 1). The N-donor ligands seem to favor shorter distances for the same bond angle than the C-donor ligands, probably a result of the more ionic bond character that allows for a larger localization of the d-type molecular orbitals and a correspondingly stronger metal−metal bonding.

The optimized structures for three model complexes with four monodentate ligands each have similar bond angles, close to 116° (Table 1), whereas the complex with six ammonia ligands has a larger bond angle (120°, a shorter Cr−Cr bond distance, and a higher Cr−Cr stretching frequency. In that case the Cr−N bond distances are significantly longer than in the analogous complex with four ligands.

Geometrical Constraints of Bridging Ligands. Most of the reported examples of quintuply bonded complexes contain bidentate bridging ligands; thus it is important to analyze the effects of the latter. Each relatively rigid N-donor bridging ligand can be characterized by its donor−donor distance d (Scheme 2), also referred to as the bite distance. Furthermore, the experimental Cr−N bond lengths l (between 1.98 and 2.10

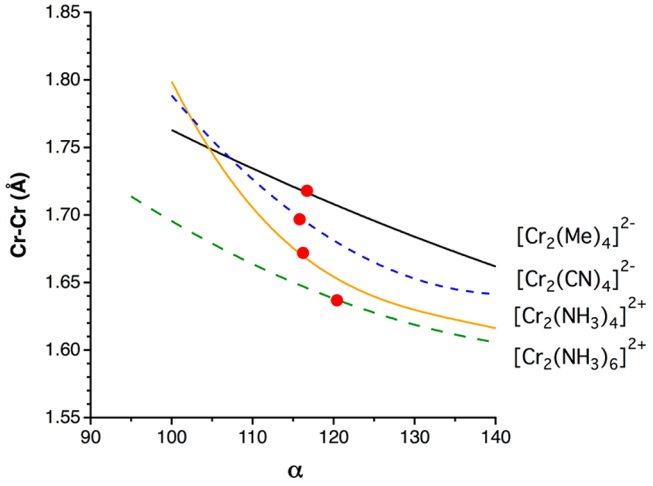

Figure 1. Cr−Cr bond distance as a function of the bond angle α (BLYP results) in complexes with monodentate ligands, with the solid circles indicating the optimized geometries.

Table 1. Geometrical Parameters and Cr−Cr Stretching Frequency (BLYP Calculations) for the Optimized Geometries of Cr(I) Complexes with Monodentate Ligands[a]

optimized	d	i	Cr−X	α	Cr−Cr	ν_{Cr-Cr}
$[Cr_2Me_4]^{2-}$	3.689	3.913	2.190	116.7	1.718	606
$[Cr_2(CN)_4]^{2-}$	3.519	3.762	2.090	115.8	1.697	621
$[Cr_2(NH_3)_4]^{2+}$	3.590	3.894	2.170	116.2	1.672	628
$[Cr_2(NH_3)_6]^{2+}$	4.527[b]	3.423	2.291	120.4	1.637	744

[a]See Scheme 2 for definitions. All distances in Å, frequencies in cm^{-1}. [b]Staggered conformation.

Å) can be considered as approximately constant at 2.04 Å. Although our calculated values for simple model complexes (Table 1) give longer bond distances, we will show in the

DOI: 10.1021/acs.inorgchem.5b02059
Inorg. Chem. 2015, 54, 10966−10977

Scheme 2. Geometrical Parameters of Cr_2L_2 Complexes with Bridging Ligands

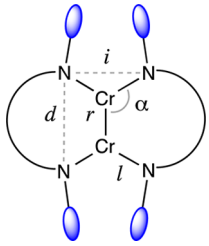

discussion below that the discrepancy is due to the much wider bond angles adopted by the monodentate ammonia ligands. Accordingly, for ligands with the same bite distance d, the Cr−Cr bond distance must vary with the average Cr−Cr−N bond angle α (see eq 1). A further consequence of the rigidity of the bridging ligands is that the interligand N···N distance i should also be correlated with α (and hence with the Cr−Cr distance) through eq 2, a fact that may be relevant when steric hindrance of the N-substituents becomes important.

$$\text{Cr-Cr} = r = d - 2l\sin(\alpha - 90°) \quad (1)$$

$$i = 2l\cos(\alpha - 90°) \quad (2)$$

When comparing bridging ligands that differ only in the substituents at the N atoms, we may assume the bridging ligands to be fairly rigid (i.e., d approximately independent of the substituents at the N atoms), and the Cr−N distances to be practically insensitive as well to the nature of the substituents. Therefore, one should expect bulkier substituents to favor a longer interligand distance i and correspondingly smaller angles α (Scheme 3 and eq 2). Then, according to eq 1 we should also

Scheme 3. Variation of the Cr−Cr Bond Distance Supported by Two Rigid Bridging Ligands and Sterics of Substituents in Cr_2L_2 Complexes

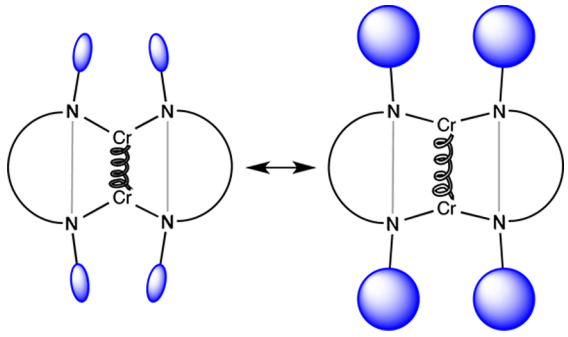

expect bulkier substituents to induce longer Cr−Cr distances. A simple way to visualize these relationships is to consider the Cr−Cr bond as a spring and the Cr−N bonds as hinges attached to a rigid ligand skeleton (Scheme 3). Assuming then that there are some geometrical constraints that force the bonding parameters α and r to be correlated, we face the challenge of trying to understand what makes each particular molecule choose a given combination of those two parameters.

If we plot eq 1 for different bite distances d alongside the results of our calculations with monodentate ligands (Figure 2a), we can see that the corresponding interligand distance d between monodentate ligands varies little in the optimized structures and appears to obey eq 1 with d = 3.6 Å and l = 2.04 Å. In the absence of the rigid constraints imposed by bridging ligands, the differences in Cr−Cr bond distances must be due to electronic reasons, given the negligible steric effects expected for the small ligands at such distance. It is interesting to note that at larger angles, the energy of the Cr_2L_4 systems increases but shorter Cr−Cr distances are favored, suggesting that a stronger Cr−Cr bond is made at the expense of disproportionally weakening the Cr−L bonds as one loses the sp^2 hybridization.

It is useful to compare the behavior of our nonbridged computational models with the experimental structures of Cr−Cr quadruple and quintuple bonds supported by bridging ligands with the NCN skeleton (Figure 2b). The resulting plot shows a continuous distribution of the structural data from the longest quadruple bonds to the shortest quintuple bonds, organized along the line that represents the geometrical relationship (eq 1) with d = 2.3 Å. A few trends seen in that plot are worth stressing: (i) The quadruple bonds cover a wide range of bond distances and present the expected correlation between bond lengths and bond angles. (ii) The quintuple bonds follow the same trend as the quadruple bonds, only at shorter Cr−Cr bond distances and correspondingly larger angles. (iii) The quintuple bonds show a comparatively small variability of the Cr−Cr distances. (iv) Among quintuply bonded compounds, those of Cr_2L_3 stoichiometry show the same behavior as the Cr_2L_2 family. (v) A compound[5] with a formal bond order of 4.5 presents a behavior intermediate between those of the quadruple and quintuple bonds.

We will see later that the use of different skeletons to support the donor atoms of the bridging ligands may affect the bite distance d as well as the rigidity of the ligand, as the number of intervening atoms and/or the degree of saturation of the skeletal bonds are varied. These factors will therefore add to the complexity of the bond angle−bond distance correlation.

Orientation of the Bridging Ligands. We have already noted that steric bulk of the N-substituents may have an influence on the choice of bond angle and bond distance, but it is worth looking at an electronic factor, namely, the directionality of the Cr−N bond relative to the ligand skeleton, which we can describe by the asymmetry between the two bond angles associated with that bond, i.e., the difference $\lambda_1 - \lambda_2$ (Scheme 4). That angular asymmetry is in part determined by the topology of the ligand, but may also be affected by steric repulsions or hydrogen bonding interactions involving the substituent R that can affect the wing angle ω. The preferred lone pair orientation of a particular uncoordinated ligand may be estimated from the position of the protons in the series of mono- and diprotonated ligands, $[H_2N(CH)_nNH]$ and $[H_2N\text{-}(CH)_nNH_2]^+$, where n = 1−3 (angle β in Scheme 4), obtained from DFT calculations.

A geometrical analysis of those computational models (Table 2 and Figure 3) indicates that the preferred geometry in the protonated ligands corresponds to an angular asymmetry $\lambda_1 - \lambda_2$ between −3 and −10°. Even if one may think that the asymmetry is underestimated in the monoprotonated models due to the existence of some degree of hydrogen bonding (see the N···N and N···H distances in Table 2) and maybe overestimated in the diprotonated form due to electrostatic repulsion between the two protons, the experimental angle asymmetry values for the coordinated amidinato and diiminato ligands in Cr_2 complexes (Table 3) are consistently and significantly out of the expected ranges. In the former case, the high positive asymmetries indicate that the ligand is forced to

DOI: 10.1021/acs.inorgchem.5b02059
Inorg. Chem. 2015, 54, 10966−10977

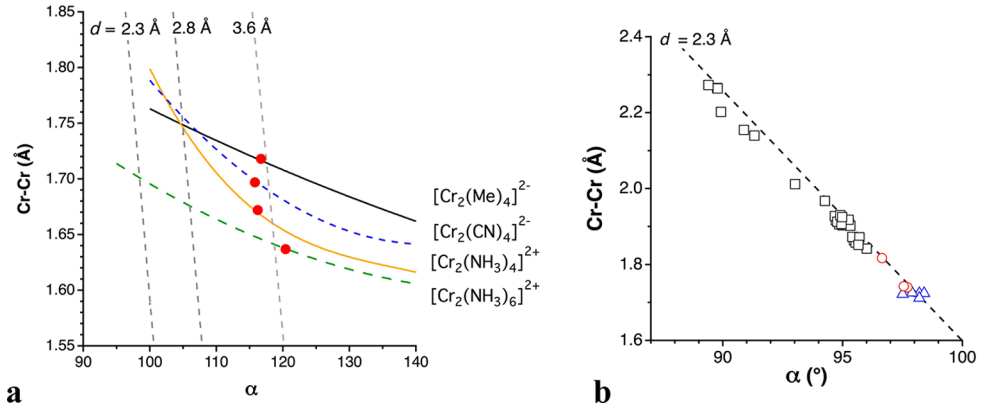

Figure 2. (a) Cr−Cr bond distance as a function of the bond angle α (BLYP results) in complexes with monodentate ligands (the solid circles indicate the optimized geometries), and the geometrical relationship between the Cr−Cr bond distance and the bond angle α (eq 1) for bridging ligands with fixed donor−donor distances noted (straight dashed lines). (b) Cr−Cr bond distance as a function of the bond angle α in experimental structures of $Cr^{II}_2L_2$ (squares), $Cr^{I}_2L_2$ (triangles), $Cr^{I}_2L_3$ and $Cr^{I}Cr^{II}L_3$ (circles) complexes.

Scheme 4. Angular Parameters, Lone Pair Orientation in Protonated Ligands and Steric Bulk of Substituents in Cr_2L_2 Complexes

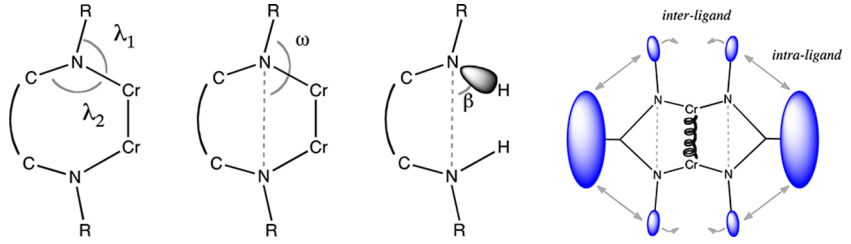

Table 2. Geometrical Parameters[a] for the Ligands Formate and $[HN(CH)_nNH]^-$, and Their Mono- and Diprotonated Forms (BLYP)[b]

ligand	X···X[c]	N···H	ω	β	$\lambda_1 - \lambda_2$
formate	2.229				
formate·H_2^+	2.316		92		
1$^-$	2.379		226		
1·H	2.332	2.532	213	89	−3
			(206−212)	(82−83)	(6−18)
1·H_2^+	2.347		213	96	−7
2$^-$	3.065		200		
2·H	2.768	2.396	178	58	−5
			(194)	(74)	(−16)
2·H_2^+	3.029		187	72	−9
3$^-$	3.330		178		
3·H	2.740	1.959	167	33	−5
3·H_2^+	3.354		167	52	−10

[a]See Scheme 4 for definitions. All distances in Å, angles in degrees. [b]Ranges of experimental values (see Table 3 for data) for Cr_2L_2 complexes given in parentheses. [c]X = O for formate, N for all other ligands.

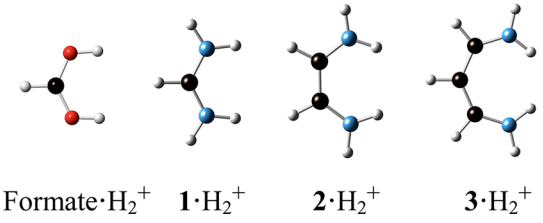

Figure 3. Optimized structures of the diprotonated ligands $[formateH_2]^+$ and $[H_2N(CH)_nNH_2]^+$ that show the variation of the orientation of the lone pair orbitals to be used to bind to chromium. Color code: C, black; O, red; N blue, H gray.

reorient the lone pairs to adequately overlap with the Cr_2 unit. The opposite situation wis obtained for the diiminato ligand, whose high negative asymmetry tells us that it is forced to reorient its lone pairs in the opposite direction, since otherwise they will be pointing to the interatomic region of the Cr_2 unit rather than to each of the chromium atoms. Only two guanidinato complexes have small asymmetry angles, and they present the two shortest Cr−Cr distances.

The possibility of affecting the orientation of the lone pairs without changing the skeleton of the bridging ligand has been successfully exploited by Kempe and co-workers.[4] Their strategy involved varying the steric bulk of the substituents in

DOI: 10.1021/acs.inorgchem.5b02059
Inorg. Chem. 2015, 54, 10966−10977

Table 3. Experimental Geometrical Parameters[a] for Quintuply Bonded Cr_2L_2 Complexes with X-Donor Ligands, and the Number of Intervening Atoms n between the Two Donors[b]

n	L[c]	X	d	Cr−X	α	Cr−Cr	ω	$\lambda_1 - \lambda_2$
2	ArNCCNAr[d]	N	2.826	1.914	104.7	1.803	196	−16
1	$C_6H_3Ar_2$[e]	C	2.477	2.223	98.3	1.839		
	$C_6H_3Ar_2$[f]	C	2.484	2.212	98.5	1.835		
	$C_6FH_2Ar_2$[g]	C	2.482	2.217	98.5	1.831		
	$C_6H_2(OMe)Ar_2$[h]	C	2.494	2.221	98.8	1.816		
	$C_6H_2(SiMe_3)Ar_2$[i]	C	2.481	2.229	98.7	1.808		
	ArAmPyAr[1][j]	N	2.275	2.013	97.5	1.750	208	9
	MesAmPyAr[2][k]	N	2.285	2.013	97.7	1.749	209	11
	Ar_2amid[l]	N	2.281	2.012	97.6	1.748	212	16
	$Ar^3{}_2$amid[m]	N	2.277	2.015	97.6	1.746	211	15
	$(ArN)_2Py$[n]	N	2.276	2.013	97.6	1.744	208	8
	Mes_2amid[o]	N	2.275	2.000	97.7	1.740	212	16
	Ar_2(Me)amid[p]	N	2.246	1.983	97.2	1.739	206	8
	Ar_2guanid[q]	N	2.268	2.018	97.7	1.729	210	4
	$Ar_2(Me_2pip)$amid[r]	N	2.242	2.007	97.6	1.706	206	−1

[a]See Scheme 4 for definitions. [b]All distances in Å, angles in degrees, frequencies in cm^{-1}. [c]Ar = $C_6H_3{}^iPr_2$; Ar^1 = 2,6-$C_6H_3Me_2$; Ar^2 = $C_6H_2{}^iPr$; Ar^3 = 2,6-$C_6H_3Et_2$ [d]CSD refcode: vitfou;[2] [e]siymuj;[16] [f]pazboi;[1] [g]siyniy;[16] [h]siyneu;[16] [i]siynaq;[16] [j]vufvic;[17] [k]hogkoe;[18] [l]xopfis01;[9e] [m]xopfue;[19] [n]tifpab;[20] [o]xopfeo;[19] [p]xopfoy;[19] [q]kuhjaz;[21] [r]wistoj.[10]

Scheme 5. Ligands Used for a Computational Prospection of Complexes with Quintuple Cr−Cr Bonds

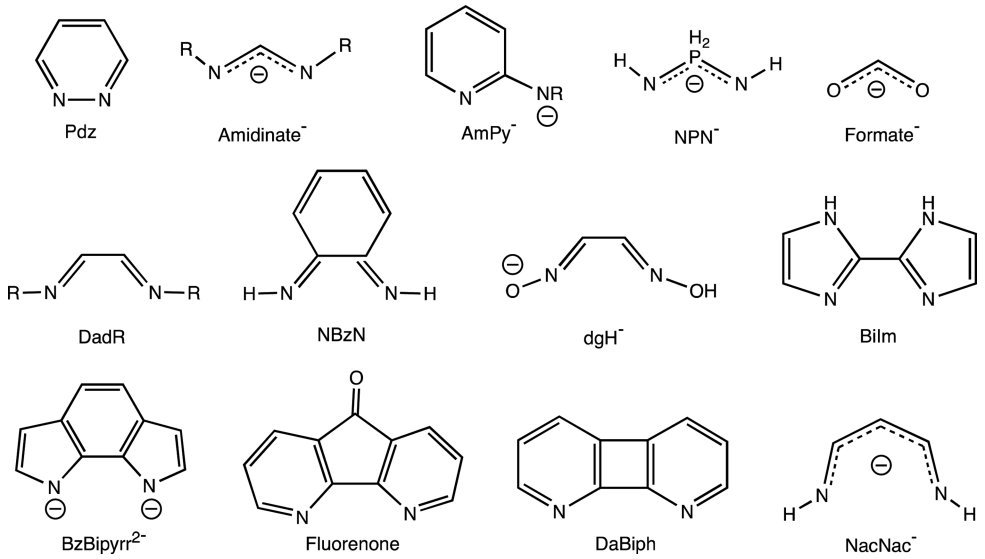

such a way as to vary the wing angle ω (Scheme 4), via intra- or interligand steric interactions. However, a look at the parameters for those complexes with amidinate and pyridylamido bridging ligands, i.e., those with one intervening carbon between the two donor atoms (Table 3), indicates that in general the wing angle ω varies little. Moreover, comparison of those angles with the corresponding values in the quadruply bonded Cr_2L_4 compounds shows that they cover similar ranges: 208−218° and 208−212° for the quadruply and quintuply bonded complexes, respectively. Moreover, no correlation is found between ω and the Cr−Cr distance within this family of compounds.

Alternative Bridging Ligands. To explore the possibilities of covering a wider range of Cr−Cr bond distances in quintuply bonded complexes, we have chosen a set of alternative bridging ligands (Scheme 5) taking into account their bite distances,[22] with the aim of varying: (a) the number of intervening atoms between the two donors, from 0 to 3 (experimentally only one or two spacer atoms have been incorporated so far), (b) the topology of the ligand, in such a way as to force a much larger variation of the wing angle ω and angular asymmetry $(\lambda_1 - \lambda_2)$ than in the currently know complexes, (c) the number of bidentate ligands, in Cr_2L_2, Cr_2L_3, and Cr_2L_4 systems, and (d) the effect of using a different set of donor atoms. The abbreviations used for those ligands throughout this paper are given in Scheme 5 in order of increasing intervening atoms between the two donors: with n = 0, pyridazine (Pdz); with n = 1, amidinate$^-$, pyridylamide ($AmPy^-$), diamidophosphonate (NPN^-), and formate$^-$; with n = 2, 1,4-diazadiene and its monoanion (DadR and $DadR^-$), *o*-benzoquinonediimine (NBzN), dioximato (dgH^-), bisimidazole (BiIm), benzobipyrrolato ($BzBipyrr^{2-}$), fluorenone, and 1,8-diazabiphenylene (DaBiph), and with n = 3, 1,3-diketiminate ($NacNac^-$).

The results of our calculations on this set of complexes are summarized in Table 4. The agreement between the calculated (Table 4) and the related experimental structures (Table 3)—where available—is excellent, with deviations smaller than 2° in the angle α and 0.03 Å in the Cr−Cr distance. The BLYP

DOI: 10.1021/acs.inorgchem.5b02059
Inorg. Chem. 2015, 54, 10966−10977

Table 4. Calculated (BLYP) Geometrical Parameters[a] and Stretching Frequencies for Cr_2L_2 Complexes with the Ligands Shown in Scheme 5, Ordered According to the Number of Intervening Atoms n between the Two Donors[b]

n	L[c]	d	i	Cr−X	α	Cr−Cr	$\lambda_1 - \lambda_2$	ω	ν_{Cr-Cr}
3	NacNac$^-$	3.161	3.569	1.920	109.9	1.851	−41.5	175	557
2	*DadH$^-$	2.819	3.707	1.927	105.9	1.762	−16.0	190	595
	DadAr$^-$	2.914	3.755	1.957	106.4	1.774	−11.4	193	541
	*NBzN	2.792	3.779	1.959	105.3	1.760	−21.8	189	583
	dgH$^-$	2.838	3.790	1.970	105.9	1.758	−21.5	186	555
	*DadH	2.819	3.861	2.004	105.6	1.743	−17.6	190	577
	BzBipyrr^{2-}	3.095	3.863	2.051	109.6	1.716	9.8	203	591
	fluorenone	3.071	3.610	2.074	109.2	1.710	−4.3	190	586
	BiIm	2.930	3.898	2.043	107.4	1.708	−4.9	197	605
	DaBiph	3.379	3.939	2.140	113.1	1.703	28.2	205	539
1	*amid$^-$	2.279	3.985	2.012	97.9	1.726	18.0	214	608
	Ar_2amid$^-$[d]	2.299	4.004	2.022	98.2	1.724	14.7	209	614
	$Ar^1{}_2$guanid$^-$[e]	2.298	4.049	2.046	98.2	1.712	5.7	208	629
	Ar_2AmPy$^-$[f]	2.322	3.989	2.013	98.4	1.724	13.0	209	610
	NPN	2.626	3.998	2.051	102.9	1.707			622
0	*Pdz	1.371	4.285	2.148	85.7	1.692	51.0	240	630

[a]See Scheme 4 for definitions of geometrical parameters. [b]All distances in Å, angles in degrees, frequencies in cm^{-1}. [c]Ar = 2,6-$C_6H_2Me_3$; Ar^1 = 2,6-$C_6H_3{}^iPr_2$; $Ar^2{}_2$ = 2,4,6-$C_6H_2{}^iPr_3$; for other abbreviations see Scheme 5. The compounds marked with an asterisk have been the object of a detailed analysis of the composition of their metal−metal bonding MOs. [d]CSD refcode of related experimental structure: xopfeo,[19] [e]kuhjaz,[21] [f]hogkoe.[18]

functional was chosen because of its better agreement with experimental data than other functionals tested. A plot of the calculated Cr−Cr bond length as a function of the Cr−Cr−X bond angle α (Figure 4) allows us to obtain a first perspective

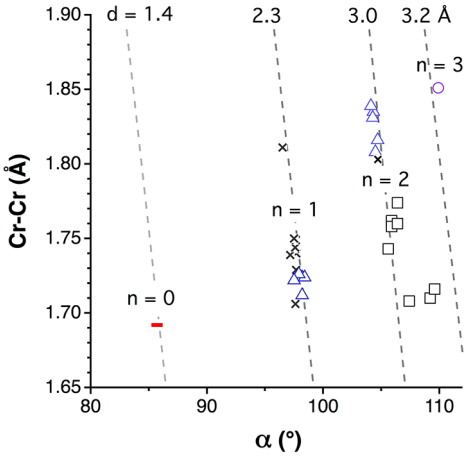

Figure 4. Calculated Cr−Cr bond distances (BLYP) as a function of the Cr−Cr−N bond angle α, classified by the number of intervening atoms between the two donors, n = 0 (bar), 1 (triangles), 2 (squares), 3 (circle). Dashed lines correspond to eq 1 for the bite distances d indicated on top, experimental data also shown for comparison (crosses).

of the variability in bonding and geometry within this family of compounds. First we observe that the range of expected Cr−Cr bond distances, 1.69−1.85 Å, may slightly expand the currently known values for compounds with N-donor ligands (1.71−1.84 Å, Scheme 1). Second, the data are roughly organized according to the values of the bite distance d, following eq 1, and the dispersion of points with different α values but similar Cr−Cr distances can be attributed to differences in their d values. Finally, it seems that a larger number of intervening carbon atoms increases the bond angle and the Cr−Cr distance, although there is no clear correlation.

Comparison of the different computational models with n = 2 reveals that the group of structures with shorter Cr−Cr distances have positive angular asymmetries $\lambda_1 - \lambda_2$, in the range 4−28°, whereas those with longer Cr−Cr distances have negative values, between −11 and −22°. If we replot the calculated and experimental Cr−Cr distances as a function of the angular asymmetry parameter $\lambda_1 - \lambda_2$ (Figure 5a) we find now that the angular asymmetry is strongly dependent on the ligand topology, but a fair correlation accounts for some of the bond distance variability. The point that deviates most from the general trend (not shown in Figure 5a) corresponds to the only compound with additional axial ligands, $[Cr_2(amidinato)_2(thf)_2]$,[20] which presents a much longer Cr−Cr distance (1.81 Å) than other complexes with similar asymmetry ($\lambda_1 - \lambda_2$ = 15°).

At the same time we observe that the opposite trend is found for the Cr−N bond distances, which increase in an approximately linear way as the angular asymmetry becomes more positive. It is now straightforward to conclude that a compensation exists between the Cr−N and Cr−Cr bonds: a high negative angular asymmetry favors stronger Cr−N bonds at the expense of weakening the Cr−Cr bond, while a high positive angular asymmetry results in weaker Cr−N bonds, asymptotically strengthening the Cr−Cr bond, which may reach distances close to that for the unperturbed Cr_2^{2+} cation (1.600 Å at the computational level used throughout this paper). The correlation between the two bond distances, seen in Figure 5b, presents an entirely different behavior from the quadruply bonded Cr^{II} analogues.

The poorer correlation between the angular asymmetry and the Cr−Cr distance (Figure 5a), compared to that between the two sets of bond distances (Figure 5b), is probably because the strength of the Cr−N bond also depends on the degree of lone pair localization at the N atom. Indeed, an excellent linear correlation is found between α and the Cr−N bond distance for the calculated structures, except for the aromatic ligands (fluorenone, BiIm, $BzBipyrr^{2-}$, and DaBiph), which strongly deviate from the general behavior, and the available experimental data follow the same trend. It must be stressed

DOI: 10.1021/acs.inorgchem.5b02059
Inorg. Chem. 2015, 54, 10966−10977

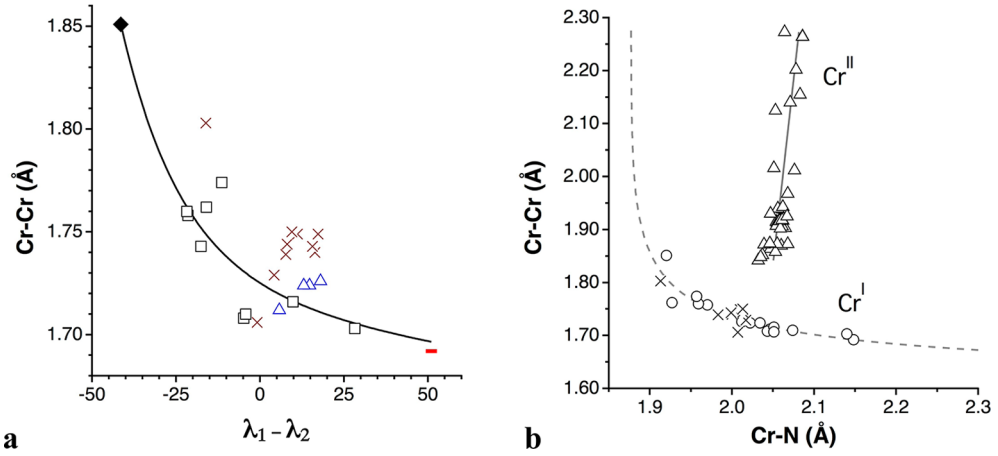

Figure 5. (a) Calculated (symbols as in Figure 4) and experimental (crosses) Cr−Cr bond distances as a function of the lone pair angular asymmetry, $\lambda_1 - \lambda_2$, for Cr(I) complexes with quintuple bonds and varying number of intervening atoms between the two donors. (b) Relationship between Cr−N and Cr−Cr quintuple bond distances in the optimized (circles) and experimental (crosses) structures, and experimental data for quadruply bonded analogues (triangles).

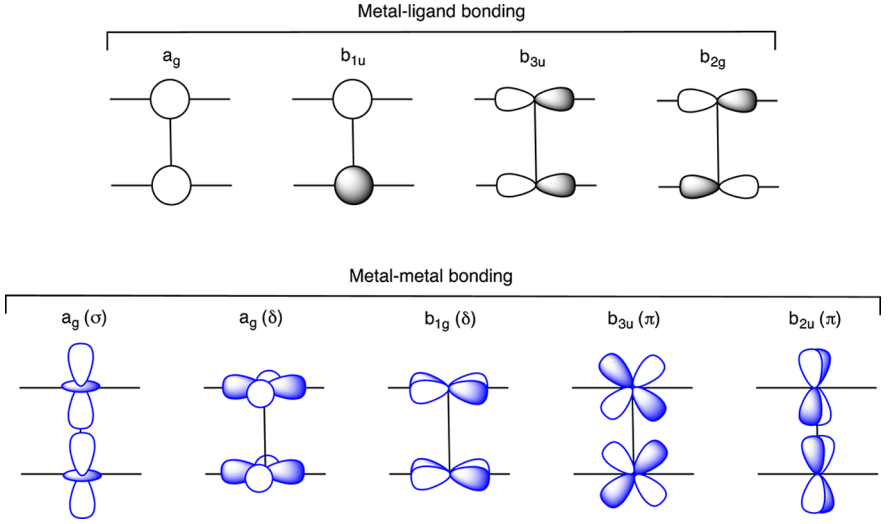

Figure 6. D_{2h} symmetry-adapted combinations of the metal atomic orbitals that participate in metal−ligand and metal−metal bonding in a quintuply bonded Cr_2L_2 complex, disregarding hybridization. The five d-block orbitals are doubly occupied.

that the data from the experimental structures also fit nicely into the trend found for the calculated structures, with the exception of the already mentioned amidinato complex with two tetrahydrofuran molecules coordinated at axial positions. The exponential correlation found means that the Cr−N bond distances vary little in compounds with longer Cr−Cr distances, but are highly sensitive to small variations at Cr−Cr distances shorter than ca. 1.72 Å. It is also interesting to see that the relationship between the two bond distances apparently follows the opposite trend for related quadruply bonded complexes (Figure 5b), where small increases in the Cr−N distances are associated with a large increase of the Cr−Cr bond length.

Given the apparent shortening of the Cr−Cr bond distance as the Cr_2L ring size decreases (i.e., as n decreases), it is natural to ask what will happen when we use a single atom-bridge. Extrapolating to a still smaller bridging skeleton, we can consider single atom-bridged Cr_2X_2 complexes (X = amide, halide), some of which have been studied earlier in detail by Merino et al.,[9c] who found a Cr−Cr distance of 1.69 Å for the Cr_2Br_2 molecule. With the methodology used in this work, we have found minima at slightly shorter distances, namely, 1.662, 1.661, and 1.659 Å for X = NH_2, Br, and Cl, respectively (stretching frequencies 758, 722, and 732 cm^{-1}). The analogous fluoride-bridged complex was found to not be a minimum, corresponding rather to a linear F−Cr−Cr−F molecule with a still shorter distance of 1.612 Å and a stretching mode at 917 cm^{-1}. These distances approach the likely limit of 1.600 Å calculated for an independent Cr_2^{2+} ion. Moreover, we observe that the ranges of Cr−Cr distances and Cr−Cr−L bond angles calculated for complexes with ligands of different sizes, including the Cr_2X_2 ones, show a smooth dependence on the number of intervening bonds between the two bridging donor atoms, with the exception of the largest ligand analyzed ($NacNac^-$). This fact provides further confirmation that in the $NacNac^-$ ligand a serious orbital mismatch, as calibrated by a large negative asymmetry parameter ($\lambda_1 - \lambda_2$, Table 4), accounts for a poorer Cr−Cr bonding than would be expected from geometric considerations.

Orbital Analysis. To unravel the orbital reasons for the compensation between metal ligand and metal−metal bonding in the Cr_2L_2 complexes, we focus on the nine symmetry-

DOI: 10.1021/acs.inorgchem.5b02059
Inorg. Chem. 2015, 54, 10966−10977

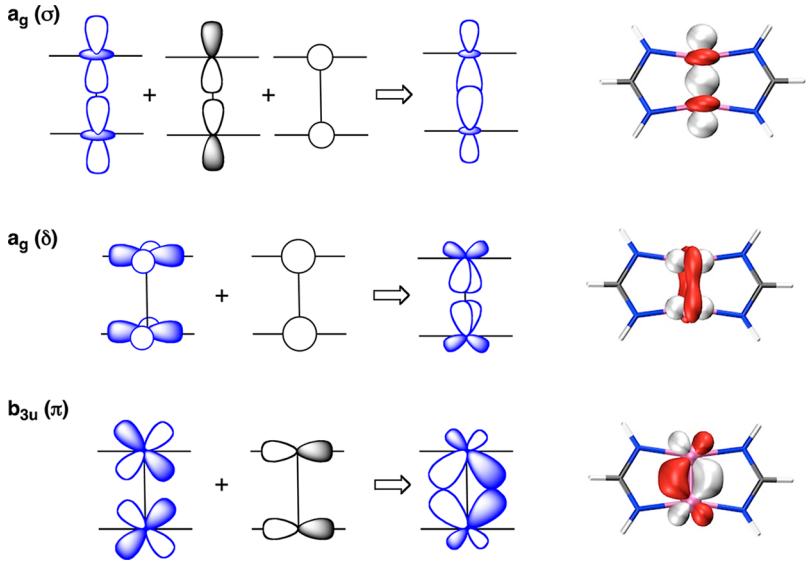

Figure 7. Schematic depiction of the hybridization of Cr−Cr bonding d-block molecular orbitals (blue) with the metal s and p orbitals (black) for Cr_2L_2 complexes, and isocontour plots of the corresponding orbitals as obtained from DFT calculations on $[Cr_2(amidinato)_2]$.

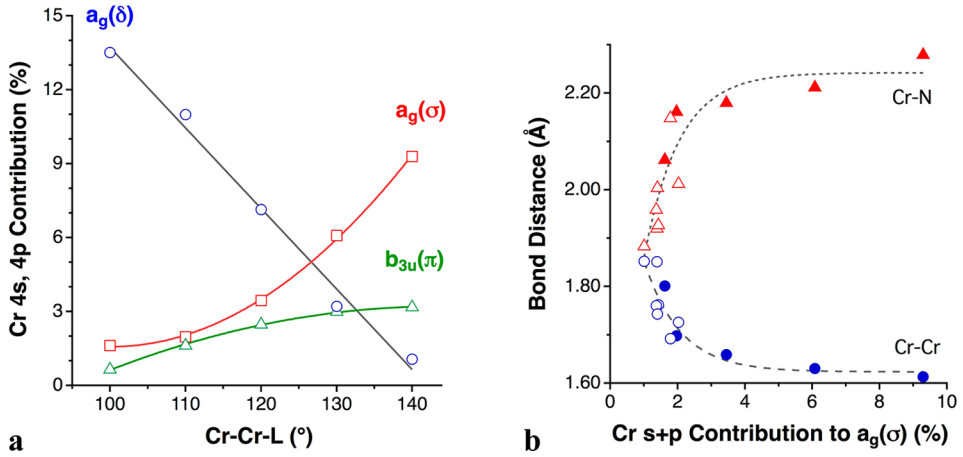

Figure 8. (a) Effect of the Cr−Cr−L bond angle on the hybridization of the Cr−Cr bonding MOs shown in Figure 7 for the model complex $[Cr_2(NH_3)_4]^{2+}$ and (b) relationship between calculated Cr−Cr (circles) and Cr−N (triangles) bond distances and the contribution of the Cr 4s and 4p orbitals to the $a_g(\sigma)$ bonding MO in the model complex at different bond angles (filled symbols) and in compounds marked with an asterisk in Table 4 (empty symbols).

adapted combinations of the metal atomic orbitals involved in M−L and M−M bonding, disregarding hybridization of the d orbitals in a first approximation (Figure 6). Four of these combinations, consisting of empty s and p orbitals, are involved in metal−ligand bonding as acceptor orbitals with a formal sp (for linear CrL_2 fragments) or sp^2 (bent fragments) hybridization. Two combinations of p orbitals (b_{2u} and b_{3g}, not shown in Figure 6) are empty and suitable only for π-donation from the ligands. The five d-based MO's, doubly occupied in chromium(I) compounds, represent the σ, π, and δ components of the quintuple bond.

Since there are four metal-based orbitals of A_g symmetry (the three shown in Figure 6 plus the bonding combination of the p_z atomic orbitals), they can hybridize in such a way as to achieve the maximum possible stability of the occupied d-type MOs by reducing the lobes oriented toward the ligands and making them less antibonding.[23] At the same time, mixing of the 4s and 4p orbitals with the σ, π, and δ Cr−Cr bonding orbitals of the same symmetry enhances the metal−metal bonding, as schematically shown in Figure 7. It is worth noting that the $a_g(\delta)$ MO acquires σ-bonding character through hybridization. Also the metal−metal bonding character of $b_{3u}(\pi)$ is enhanced through hybridization with a p orbital. As for the $b_{2u}(\pi)$ orbital, its bonding-enhancing hybridization involves a π-based MO that is not involved in σ bonding with the ligands due to its nodal properties. Hence, one can anticipate that this orbital will be insensitive to changes in the Cr−Cr−L bond angle. A similar reasoning applies to the $b_{1g}(\delta)$ MO (Figure 6).

We have performed a detailed analysis of the composition of the metal−metal bonding MOs in the model $[Cr_2(NH_3)_4]^{2+}$ at various Cr−Cr−N angles (with the rest of the molecule optimized) and of the set of calculated complexes with ligands having different numbers of spacers in-between the two donor atoms, with correspondingly varied Cr−Cr−L bond angles, Cr−Cr bond distances, and Cr−L bond distances (compounds marked with an asterisk in Table 4). The hybridization schemes just discussed are substantiated by this analysis, revealing a strong hybridization of the $a_g(\delta)$ MO in the complexes with

DOI: 10.1021/acs.inorgchem.5b02059
Inorg. Chem. 2015, 54, 10966−10977

bridging ligands of varied topology, with a participation of the chromium 4s orbital of 9−16%, which introduces a significant σ-bonding character to this orbital, as shown in Figure 7 and noticed previously by Landis and Weinhold.[24]

In addition, a survey of the effect of the Cr−Cr−N bond angle in the $[Cr_2(NH_3)_4]^{2+}$ model shows a strong influence on the extent of those hybridizations (Figure 8a). In the case of the $a_g(\sigma)$ and $b_{3u}(\pi)$ MOs, the hybridization increases with increasing bond angle (i.e., a positive pyramidality effect), as previously established for quadruply bonded systems.[13a,b] However, the hybridization of the $a_g(\delta)$ MO exhibits a strong negative pyramidality effect throughout the range of bond angles explored. It is important to recall that the 4s and 4p orbitals are involved in Cr−N bonding through a formal sp^2 hybridization. Consequently, increased hybridization of the d-type MOs by mixing in 4s and 4p weakens the bonding interaction of the latter with the donor atoms, thus accounting for the compensating effect of the Cr−Cr and Cr−N bond distances.

Our analysis of compounds with bridging ligands revealed several different effects, and no simple correlations involving the Cr−Cr−N angle can be established for them. However, the degree of hybridization of the $a_g(\sigma)$ orbital can still be seen to play a major role in Cr−Cr and Cr−N bonding (Figure 8b), with the former being reinforced and the latter weakened as the degree of hybridization increases. Such hybridization consists of comparable contributions of 4s and 4p atomic orbitals, becoming predominantly 4p at small angles. Remarkably, even in those cases in which the contribution of the metal 4p atomic orbitals to the $a_g(\sigma)$ MO is rather small, it suffices to induce a non-negligible hybridization of the z^2 orbitals and strongly affect the metal−ligand and metal−metal bond strengths. In other words, at small bond angles the Cr−Cr bond is strengthened at the expense of weakening the Cr−N bonds and vice versa. This conclusion is confirmed by a nice inverse correlation between the Cr−Cr and Cr−N bond distances, as found above for the experimental structures (Figure 5b).

Some competition between δ Cr−Cr and Cr−N bonding had been noted earlier by Gagliardi.[9a] Our present analysis, however, goes further by including the angle dependence of σ, π, and δ components of the quintuple bond and establishing the role of 4s and 4p admixture on the 3d-based MOs, which combines opposing positive σ- and π- with negative δ-pyramidality effects. The negative pyramidality effect of the δ orbital may help explain the much less clearer overall pyramidality dependence of the Cr−Cr quintuple bond lengths, as well as the much narrower range of Cr−Cr bond distances compared to the analogous quadruple bonds (see Figure 2b).

In spite of the different topology and donor characteristics of the aryl ligands in Power's compounds (Scheme 1a), the hybridization of the atomic orbitals at the Cr_2^{2+} core should follow the same rules deduced for N-donor ligands, since it is clear now that the flanking arene interaction with the Cr atom consists indeed of a π coordination[25] that renders a similar CrL_2 coordination environment for each chromium atom. The Cr−Cr and average Cr−C distances vary little among the known structures of this family, but the fact that they present much longer Cr−Cr bond distances than in complexes with N-donor ligands is consistent with the more covalent character of the Cr−C bonds that should account for decreased metal contributions and, consequently, weaker Cr−Cr bonds.

Number of Bridging Ligands and Choice of Donor Atoms. We reasoned that the use of more electronegative donor atoms than nitrogen might result in a higher localization of the Cr−Cr bonding MOs at the chromium atoms. Therefore, we have replaced the amidinato ligands by its topologically equivalent O-donor, the formate anion. At the same time, we have explored with these two ligands the effect that the number of ligands has on the Cr−Cr distance by comparing the Cr_2L_2, Cr_2L_3, and Cr_2L_4 complexes. Moreover, to test the importance of steric congestion, we have used two versions of the amidinato ligand, with hydrogen or xylyl groups attached to the N-donor atoms.

The results are shown in Table 5. The geometric and vibrational parameters for the related complexes with amidinato and formato ligands are rather similar, in good agreement with their similar lone pair orientations and bite distances (Figure 3 and Table 2). The results are also similar for systems with two or three bridging ligands (vide infra), in agreement with the experimental behavior of the doubly and triply bridged amidinato complexes.[5,18] The addition of a fourth bridge, however, results in a dramatic lengthening of the Cr−Cr bond with both the amidinato and formato ligands, which we attribute to the involvement of one δ-bonding orbital in metal−ligand bonding. In contrast, the triply bridged complexes can still use the empty metal p orbitals that are not directly involved in the case of Cr_2L_2, and no significant loss of metal−metal bonding seems to accompany the addition of the third bridging ligand. Notice that, contrary to our expectations, the higher electronegativity of the donor atoms in the formate complexes compared to the N-donors of the amidinato compounds does not seem to have a significant effect on the strength of the Cr−Cr quintuple bonds.

Table 5. Calculated (BLYP) Geometrical Parameters and Stretching Frequencies for Cr_2L_n Complexes (n = 2−4) with Topologically Equivalent N- and O-Donor Ligands[a]

L_n	d	α	Cr−X	Cr−Cr	ν_{Cr-Cr}	ref
$amid_2$	2.279	2.012	97.9	1.726	608	
$(Ar_2amid)_2$	2.299	2.022	98.2	1.724	614	
Ar_2AmPy_2	2.322	2.013	98.4	1.724	610	
Ar_2AmPy_2 exp.	2.285	2.013	97.6	1.749		18
$formate_2$	2.245	1.994	97.5	1.722	615	
$amid_3$	2.289	2.054	97.5	1.754	548	
$(Ar_2amid)_3$	2.333	2.135	98.0	1.730	554	
$(Ar_2amid)_3$ exp.	2.306	2.091	97.6	1.740		5
$formate_3$	2.260	2.094	97.4	1.722	594	
$amid_4$	2.278	2.060	96.0	1.844	494	
$formate_4$	2.287	2.105	95.2	1.898	455	

[a]All distances in Å, angles in degrees, frequencies in cm^{-1}.

Capping Ligands. We have seen that among all the analyzed compounds the shortest calculated distance corresponds to Cr_2F_2 with ligands only at axial positions, and that complexes with terminal ligands exhibit shorter Cr−Cr distances than those with bridging ligands. We have therefore explored an alternative approach consisting in arranging bi- or tridentate ligands in a terminal rather than in a bridging mode, as in a chest expander (Figure 9). It may not be straightforward to synthesize quintuply bonded complexes with such geometries, even if they may emerge as energy minima in our calculations, but it is likely that adequate synthetic strategies could be developed. By using small bite angle ligands, one

DOI: 10.1021/acs.inorgchem.5b02059
Inorg. Chem. 2015, 54, 10966−10977

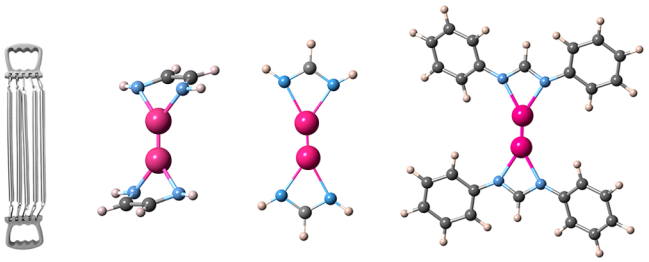

Figure 9. Chest expander topology found in the optimized structures of (from left to right) $[Cr_2(DadH)_2]$, $[Cr_2(amidinato)_2]$, and $[Cr_2(Ph_2\text{-amidinato})_2]$ with capping bidentate ligands in their singlet spin state.

could force large bond angles α and take advantage of the pyramidality effect evidenced for monodentate ligands, while avoiding the geometrical dependence between α and the Cr−Cr distance imposed by bridging ligands.

As capping tridentate ligands we have chosen the popular trispyrazolylborate (Tp) and triazacyclononane (tacn), as well as the cyclopentadienide ring (Cp), for which three "lone pairs" are in close proximity, making it equivalent to a tridentate ligand with a very small bite angle[22] that might favor a strong metal−metal bond. The topology of a metal−metal bonded complex capped with two Cp rings is not that strange, since it appears in the first compound with a Zn^I-Zn^I bond[26] $[Zn_2Cp^*_2]$ and later analogues.[27]

Some geometrical and bonding parameters of the optimized structures are given in Table 6, together with those for analogous complexes with monodentate NH_3 ligands for comparison. We can see that both the bi- and tridentate capping ligands enforce larger pyramidality angles than obtained with monodentate ligands; therefore the Cr−Cr distances, clearly affected by the bond angle, are predicted to be shorter than those experimentally characterized so far. Consistently, higher Cr−Cr stretching frequencies are predicted. The compound with an α-diiminate ($DadH^-$) ligand (Figure 9) prefers a side-on coordination, probably leaving room for relatively bulky substituents at the N atoms to provide sterical protection of the Cr−Cr bond without introducing severe ligand−ligand repulsions.

One such compound has already been realized experimentally by Kempe and co-workers, with two guanidinato ligands bearing bulky $(^i Pr)_2Ph$ groups at the N donor atoms,[10] and it is worth comparing the reported structure with the results of our calculations on complexes with amidinato, phenyl-substituted amindinato or $(^i Pr)_2Ph$-substituted guanidinato ligands. In the case of the latter complex, we have introduced dispersion corrections in our calculations to better calibrate the weakly attractive van der Waals interactions involving the isopropyl groups of the two ligands.[28] In our calculations on these three complexes at their singlet state that is compatible with a Cr−Cr quintuple bond, distances of around 1.62 Å are predicted, while the experimental bond distance is a long 2.65 Å. Calculations for the high spin state ($S = 4$) however, corresponding to a formal single Cr−Cr bond and a $\sigma^2\pi^2\delta^2\delta^{*2}\pi^{*2}$ electron configuration, predict also a long distance (2.72−2.79 Å). In the case of the bulky guanidinato complex, calculations yield the singlet state at 17.8 kcal/mol below the $S = 4$ spin state. Taken together, these results are consistent with the long experimental distance experimentally found at 193 K and with a magnetic moment that decreases with decreasing temperature, approaching zero at low temperature. The possible existence of a spin crossover behavior and the associated structural changes in this compound certainly deserves further attention from both the experimental and theoretical viewpoints.

Computational Details. All the optimizations have been obtained at the DFT level with the Gaussian 09 program.[29] Different hybrid functionals have been tested, and the BLYP exchange-correlation functional was found to give the best results, close to experimental data. The analysis of the vibrational frequencies has been done on the optimized geometries and within the harmonic approximation. The TZVP basis set[30] was used for all atoms. In calculations for $[Cr_2((i Pr_2Ph)_2\text{guanidinato})_2]$ the empirical dispersion terms of

Table 6. Calculated (BLYP) Geometrical Parameters and Stretching Frequencies for Cr_2L_2 Complexes with X-donor Bi- and Tridentate Capping Ligands[a]

	Cr−X	α	Cr−Cr	ν_{Cr-Cr}
$[Cr_2(NH_3)_4]^{2+}$	2.170	116.2	1.672	628
$[Cr_2(NacNac)_2]$	2.020	130.2	1.664	668
$[Cr_2(DadH)_2]$	1.983	134.6	1.680	700
$[Cr_2(amidinate)_2]$, $S = 0$	2.138	148.0	1.619	829
$[Cr_2(amidinate)_2]$, $S = 4$	2.029	122.6	2.793	166
	2.200	164.4		
$[Cr_2(Ph_2amidinate)_2]$, $S = 0$	2.142	148.0	1.621	829
$[Cr_2(Ph_2amidinate)_2]$, $S = 4$	2.06−2.20	126−153	2.782	229
$[Cr_2((iPr_2Ph)_2guanidinate)_2]$, $S = 0$[f]	2.098	146	1.624	821
$[Cr_2((iPr_2Ph)_2guanidinate)_2]$, $S = 4$[f]	2.08	141	2.721	260
$[Cr_2((iPr_2Ph)_2guanidinate)_2]$,[10] exp.	2.040	147.0	2.652	
$[Cr_2(NH_3)_6]^{2+}$[d]	2.291	120.4	1.637	744
$[Cr_2Tp_2]$[d]	2.136	124.9	1.657	678
$[Cr_2(tacn)_2]^{2+}$	2.244	132.2	1.635	778
$[Cr_2Cp_2]$[e]	2.335	148[b]	1.629	810[c]

[a]All distances in Å, angles in degrees, frequencies in cm^{-1}. [b]The effective angle α for Cp considered as a tridentate capping ligand has been obtained from the ring size and the average Cr−C bond distances[22] and is comparable to that deduced earlier from a wide sample of structures (10.000 data) with η^5-Cp rings (145°). [c]One imaginary frequency of −2 cm^{-1} corresponds to the rotation of one Cp ring relative to the other. [d]Staggered conformation. [e]Eclipsed conformation. [f]Dispersion included.

DOI: 10.1021/acs.inorgchem.5b02059
Inorg. Chem. 2015, 54, 10966−10977

Grimme were introduced using the corresponding BLYP-D functional[31] to better calibrate the interligand interactions.

CONCLUSIONS

Our calculations on simple model chromium(I) complexes with monodentate ligands indicate that these—currently hypothetical—molecules show a correlation between bond angle (α) and bond distance, and the optimized geometries suggest that shorter Cr−Cr distances than currently known might be achievable. Apparently more covalent chromium−ligand bonds result in longer Cr−Cr bonds.

In Cr_2L_2 complexes with relatively rigid N-donor bridging ligands, a linear relationship between bond angle α and Cr−Cr bond distance is determined by the approximately constant N···N bite distance and Cr−N bond lengths, and both bonding parameters may adjust to the steric requirements of the substituents. For ligands with a RNCNR backbone, that same correlation organizes the structural data of both chromium(II) quadruply bonded and chromium(I) quintuply bonded complexes. A more important effect is associated with changes in the lone pair orientation, and with changes in the degree of localization of those lone pairs determined by modifications of the ligand backbone. These effects are made evident by a strong dependence of the Cr−Cr bond distance on the degree of angular asymmetry of the two Cr−N-R bond angles at the donor atom (a direct result of a mismatched lone pair orbital orientation) and by an inverse correlation between Cr−N and Cr−Cr bond distances.

As corollary of the trends just discussed, a rough tendency emerges, predicting shorter Cr−Cr distances on average for ligands with smaller numbers of intervening bonds between the two donors. Thus, a pyridazine-bridged chromium(I) complex is predicted by our calculations to have a record short Cr−Cr distance of 1.69 Å. Extrapolating to a still smaller bridging skeleton, the single atom-bridged ligands in Cr_2X_2 complexes (X = amide, halide) favor still shorter Cr−Cr distances, at around 1.66 Å. Altogether, the experimental and calculated complexes present an inverse exponential correlation between the Cr−Cr and Cr−N bond distances.

Our orbital analysis of Cr_2L_4 complexes with monodentate and Cr_2L_2 with bridging bidentate ligands supports an idealized bonding model that implies the use of sp^2 hybrid orbitals at the chromium atoms for Cr−N bonding and of the five 3d orbitals for Cr−Cr bonding.[9b] However, hybridization of the metal−metal bonding MOs through mixing-in of 4s and 4p orbitals strengthens these bonds at the expense of weakening the metal−ligand ones. Such hybridization confers a significant degree of σ bonding character upon a formally δ bonding MO, accounting for a stronger second δ bond than previously thought. The hybridization of these MOs depends on the Cr−Cr−L bond angle in two different ways: while the σ and π components increase their degree of hybridization upon increasing the bond angle (a positive pyramidality effect), the hybridization of the δ orbital presents a negative pyramidality effect (i.e., decreases upon increasing bond angle). This orbital behavior is in contrast with that present in the quadruply bonded Cr(II) analogues with four bridging ligands, Cr_2L_2, with only positive σ- and π-pyramidality effects, and may explain the much narrower range of Cr−Cr bond distances found for quintuple bonds.

The substitution of the N-donor by more electronegative oxygen atoms does not seem to have a significant effect on the bonding and vibrational parameters. Nor does the presence of bulky aryl substituents at the N atoms of the Cr_2L_2 complexes affect the Cr−Cr bond, but in the more sterically congested Cr_2L_3 analogues the bulky substituents favor a longer Cr−N and a shorter Cr−Cr distance, consistent with the compensating effect found between these two types of bonds. The addition of a fourth bridging ligand is predicted to result in a significant weakening of the Cr−Cr bond, consistent with some involvement of one of the δ orbitals in metal−ligand bonding, at the expense of weakening the Cr−Cr bond.

Finally, we have explored an alternative strategy to strengthen the Cr−Cr bond, by coordinating bi- or tridentate ligands in a capping rather than in a bridging mode. In this way, the large Cr−Cr−L bond angles enforced by small bite angle ligands favor rather short Cr−Cr distances, approaching what seems to be a lower limit of 1.60 Å. A nice correlation between bond length and stretching frequency holds for all the calculated structures, including both bridged and capped complexes (Supporting Information). We are convinced that following different design strategies than used up to now new interesting structural and reactivity features of quintuply bonded complexes will be reported in the near future.

ASSOCIATED CONTENT

Supporting Information

The Supporting Information is available free of charge on the ACS Publications website at DOI: 10.1021/acs.inorgchem.5b02059.

Tables of atomic orbital contributions to the Cr−Cr bonding orbitals, atomic coordinates for the optimized structures reported, and correlation between the Cr−Cr bond lengths and the stretching frequencies for all calculated complexes (PDF).

AUTHOR INFORMATION

Corresponding Authors

*(S.A.) E-mail: santiago@qi.ub.es.

*(K.H.T.) E-mail: theopold@udel.edu.

Notes

The authors declare no competing financial interest.

ACKNOWLEDGMENTS

This work was supported by the Spanish Ministerio de Economía y Competitividad (Project CTQ2011-23862-C02-02) and by the Generalitat de Catalunya (Project 2009SGR-1459). The experimental work in the laboratory of K.H.T. was supported by the U.S. National Science Foundation (CHE-0616375). K.H.T. thanks the Universitat de Barcelona for hosting him during a sabbatical semester in the spring of 2013.

REFERENCES

(1) Nguyen, T.; Sutton, A. D.; Brynda, M.; Fettinger, J. C.; Long, G. J.; Power, P. P. *Science* **2005**, *310*, 844−847.

(2) Kreisel, K. A.; Yap, G. P. A.; Dmitrenko, O.; Landis, C. R.; Theopold, K. H. *J. Am. Chem. Soc.* **2007**, *129*, 14162−14163.

(3) Harisomayajula, N. V. S.; Nair, A. K.; Tsai, Y.-C. *Chem. Commun.* **2014**, *50*, 3391−3412.

(4) Wagner, F. R.; Noor, A.; Kempe, R. *Nat. Chem.* **2009**, *1*, 529−536.

(5) Tsai, Y.-C.; Hsu, C.-W.; Yu, J.-S. K.; Lee, G.-H.; Wang, Y.; Kuo, T.-S. *Angew. Chem., Int. Ed.* **2008**, *47*, 7250−7253.

(6) Tsai, Y.-C.; Chen, H.-Z.; Chang, C.-C.; Yu, J.-S. K.; Lee, G.-H.; Wang, Y.; Kuo, T.-S. *J. Am. Chem. Soc.* **2009**, *131*, 12534−12535.

DOI: 10.1021/acs.inorgchem.5b02059
Inorg. Chem. 2015, 54, 10966−10977

(7) Clouston, L. J.; Siedschlag, R. B.; Rudd, P. A.; Planas, N.; Hu, S.; Miller, A. D.; Gagliardi, L.; Lu, C. C. *J. Am. Chem. Soc.* **2013**, *135*, 13142−13148.
(8) (a) Noor, A.; Kempe, R. *Inorg. Chim. Acta* **2015**, *424*, 75−82. (b) Nair, A. K.; Harisomayajula, N. V. S.; Tsai, Y.-C. *Inorg. Chim. Acta* **2015**, *424*, 51−62. (c) Noor, A.; Kempe, R. *Chem. Rec.* **2010**, *10*, 413−416. (d) Nair, A. K.; Harisomayajula, N. V. S.; Tsai, Y.-C. *Dalton Trans.* **2014**, *43*, 5618−5638. (e) Hua, S. A.; Tsai, Y.-C.; Peng, S. M. *J. Chin. Chem. Soc.* **2014**, *61*, 9−26. (f) Ni, C. B.; Power, P. P. *Struct. Bonding (Berlin, Ger.)* **2010**, *136*, 59−111.
(9) (a) Brynda, M.; Gagliardi, L.; Roos, B. O. *Chem. Phys. Lett.* **2009**, *471*, 1−10. (b) McGrady, J. E. In *Comprehensive Inorganic Chemistry II*; Reedijk, J., Poeppelmeier, K., Eds.; Elsevier: Amsterdam, 2013; Vol. *9*, pp 321−340;. (c) Merino, G.; Donald, K. J.; D'Acchioli, J. S.; Hoffmann, R. *J. Am. Chem. Soc.* **2007**, *129*, 15295−15302. (d) Ndambuki, S.; Ziegler, T. *Inorg. Chem.* **2013**, *52*, 3860−3869. (e) Wu, L.-C.; Hsu, C.-W.; Chuang, Y.-C.; Lee, G.-H.; Tsai, Y.-C.; Wang, Y. *J. Phys. Chem. A* **2011**, *115*, 12602−12615.
(10) Noor, A.; Bauer, T.; Todorova, T. K.; Weber, B.; Gagliardi, L.; Kempe, R. *Chem. - Eur. J.* **2013**, *19*, 9825−9832.
(11) Horvath, S.; Gorelsky, S. I.; Gambarotta, S.; Korobkov, I. *Angew. Chem., Int. Ed.* **2008**, *47*, 9937−9940.
(12) (a) Ardon, M.; Bino, A.; Cohen, S.; Felthouse, T. R. *Inorg. Chem.* **1984**, *23*, 3450−3455. (b) Cotton, F. A.; Mott, G. N. *Inorg. Chem.* **1983**, *22*, 1136−1139.
(13) (a) Losada, J.; Alvarez, S.; Novoa, J. J.; Mota, F.; Hoffmann, R.; Silvestre, J. *J. Am. Chem. Soc.* **1990**, *112*, 8998−9000. (b) Mota, F.; Novoa, J. J.; Losada, J.; Alvarez, S.; Hoffmann, R.; Silvestre, J. *J. Am. Chem. Soc.* **1993**, *115*, 6216−6229. (c) Alvarez, S.; Alemany, P.; Aullón, G.; Palacios, A. A.; Novoa, J. J. In *The Synergy Between Dynamics and Reactivity at Clusters and Surfaces*; Farrugia, L. J., Ed.; Kluwer Academic: Dordrecht, 1995; pp 241−255. (d) Liu, X.-Y.; Alvarez, S. *Inorg. Chem.* **1997**, *36*, 1055−1060.
(14) Aullón, G.; Alvarez, S. *Inorg. Chem.* **1993**, *32*, 3712−3719.
(15) Aullón, G.; Alemany, P.; Alvarez, S. *Inorg. Chem.* **1996**, *35*, 5061−5067.
(16) Wolf, R.; Ni, C.; Nguyen, T.; Brynda, M.; Long, G. J.; Sutton, A. D.; Fischer, R. C.; Fettinger, J. C.; Hellman, M.; Pu, L.; Power, P. P. *Inorg. Chem.* **2007**, *46*, 11277−11282.
(17) Noor, A.; Glatz, G.; Muller, R.; Kaupp, M.; Demeshko, S.; Kempe, R. *Nat. Chem.* **2009**, *1*, 322−325.
(18) Noor, A.; Wagner, F. R.; Kempe, R. *Angew. Chem., Int. Ed.* **2008**, *47*, 7246−7249.
(19) Hsu, C.-W.; Yu, J.-S. K.; Yen, C.-H.; Lee, G.-H.; Wang, Y.; Tsai, Y.-C. *Angew. Chem., Int. Ed.* **2008**, *47*, 9933−9936.
(20) Huang, Y.-L.; Lu, D.-Y.; Yu, H.-C.; Yu, J.-S. K.; Hsu, C.-W.; Kuo, T.-S.; Lee, G.-H.; Wang, Y.; Tsai, Y.-C. *Angew. Chem., Int. Ed.* **2012**, *51*, 7781−7785.
(21) Noor, A.; Glatz, G.; Muller, R.; Kaupp, M.; Demeshko, S.; Kempe, R. *Z. Anorg. Allg. Chem.* **2009**, *635*, 1149−1152.
(22) Aguilà, D.; Escribano, E.; Speed, S.; Talancón, D.; Yermán, L.; Alvarez, S. *Dalton Trans.* **2009**, 6610−6625.
(23) Alvarez, S.; Cirera, J. *Angew. Chem., Int. Ed.* **2006**, *45*, 3012−3020.
(24) Landis, C. R.; Weinhold, F. *J. Am. Chem. Soc.* **2006**, *128*, 7335−7345.
(25) Falceto, A.; Carmona, E.; Alvarez, S. *Organometallics* **2014**, *33*, 6660−6668.
(26) Resa, I.; Carmona, E.; Gutiérrez-Puebla, E.; Monge, A. *Science* **2004**, *305*, 1136−1138.
(27) Carmona, E.; Galindo, A. *Angew. Chem., Int. Ed.* **2008**, *47*, 6526−6536.
(28) (a) Schreiner, P. R.; Chernish, L. V.; Gunchenko, P. A.; Tikhonchuk, E. Y.; Hausmann, H.; Serafin, M.; Schlecht, S.; Dahl, J. E. P.; Carlson, R. M. K.; Fokin, A. A. *Nature* **2011**, *477*, 308−311. (b) Grimme, S.; Schreiner, P. R. *Angew. Chem., Int. Ed.* **2011**, *50*, 12639−12642.
(29) *Gaussian09* (B.1), Frisch, M. J.et al. Gaussian, Inc.: Wallingford, CT, 2010.
(30) Schäfer, A.; Huber, C.; Ahlrichs, R. *J. Chem. Phys.* **1994**, *100*, 5829.
(31) (a) Grimme, S. *J. Comput. Chem.* **2004**, *25*, 1463−1473. (b) Grimme, S. *J. Comput. Chem.* **2006**, *27*, 1787−1799. (c) Grimme, S.; Antony, J.; Ehrlich, S.; Krieg, H. *J. Chem. Phys.* **2010**, *132*, 154104.

DOI: 10.1021/acs.inorgchem.5b02059
Inorg. Chem. 2015, 54, 10966−10977